Di-Alkyl Adipates as New Phase Change Material for Low Temperature Energy Storage

Maria C. M. Sequeira[1] · Bernardo A. Nogueira[2] · Fernando J. P. Caetano[1,3] · Hermínio P. Diogo[1] · João M. N. A. Fareleira[1] · Rui Fausto[2,4]

Abstract

This work is a contribution to the thermal characterization of a selected binary system of two di-*n*-alkyl adipates that can be used as phase change material for thermal energy storage at low temperatures. The construction of the solid–liquid phase diagram using differential scanning calorimetry (DSC), complemented with Raman Spectroscopy studies for the system composed by diethyl and dibutyl adipates is presented. The *solidus* and *liquidus* equilibrium temperatures were determined by DSC for the pure components and 30 binary mixtures at selected molar compositions were used to construct the corresponding solid–liquid phase diagram. The binary system of diethyl and dibutyl adipates presents eutectic behaviour at low temperatures. The eutectic temperature was found at 240.46 K, and the eutectic composition was determined to occur at the molar fraction $x_{\text{dibutyl}} = 0.46$. Additionally, the system shows a polymorphic transition, characteristic of dibutyl adipate, occurring at ca. 238 K, confirmed by optical microscopy. To the best of our knowledge, no reference to the phase diagram of the present system could be found in the literature. Raman spectroscopy was essential to complement the construction of the phase equilibrium diagram, enabling the identification of the solid and liquid phases of the system. Finally, the *liquidus* curve of the phase diagram was also successfully predicted using a suitable fitting equation, being the root mean square deviation of the data from the correlation equal to 0.54 K. In addition, this fitting operation enabled a correct prediction of the eutectic composition of the system.

Extended author information available on the last page of the article

🍂 Springer

1 Introduction

The increasing worldwide need for energy requires urgent and effective solutions. It is widely recognized that the supply of renewable energies is principally intermittent, which often leads to a disturbing gap between energy availability and its consumption. Therefore, energy storage becomes a very significant tool for increasing the efficiency in the use of the produced renewable energy. Energy Storage is thus considered to be a fundamental means to enable the transition to alternative cleaner and more efficient use of energy. As a consequence, it has received worldwide attention and increasing study interest [1].

Thermal energy storage (TES) is one of the different forms of energy storage and its use has been increasing in recent decades and one growing technology makes use of the latent heat storage, which relies on the energy involved in the phase transition, often between the solid and liquid phases of a material. Latent heat storage (LHS) became attractive as a result of some specific characteristics such as the nearly isothermal nature of the phase-change process, compactness and the high latent heat inherently involved [2–9].

Phase change materials (PCMs), are materials specifically used for latent heat storage applications [10, 11]. These materials are characterized for being able to absorb and release heat from the surroundings by changing phase, thus enabling the storage of a substantial amount of thermal energy [10, 12]. In fact, the use of PCMs for latent heat storage provides a high energy storage density due to the large amount of heat exchanged during the phase-change process. Furthermore, this exchange occurs with a small variation of the temperature of the PCM, as the temperature must remain practically constant while the two phases are in equilibrium. Additionally, the volume of the PCM does not change significantly during the solid–liquid phase-change, which is an interesting characteristic for their industrial applications; one advantage is a more efficient energy transport to a heat transfer fluid (HTF). Consequently, latent heat storage using PCMs is one of the most effective systems to store thermal energy [4], having attracted significant attention from several authors [11–17]. Additionally, the use of these materials for latent heat storage has taken a very important role, especially for active cooling systems, in particular, eutectic systems that can be customized for each application, allowing significant energy savings, being relevant to the economic and environmental sustainability [18].

Phase equilibrium studies aimed to obtain phase diagrams which are important to characterize the behaviour of PCM systems, including the desired melting temperatures, revealing their aptitude for an industrial application [19]. Differential scanning calorimetry (DSC) is one of the most effective and used techniques to determine whether binary mixtures form solid solutions or eutectic systems [1]. In fact, it is an important tool to construct solid–liquid phase diagrams for binary organic and inorganic systems [20].

In recent years, alkanes and paraffins have been under massive research because of their high latent heat enthalpy and chemical stability. However, in general, the high cost of paraffins when compared to other organic compounds

restricts their use in a wide range of applications [21]. To solve this problem, various non-paraffinic-based compounds, such as esters, fatty alcohols and fatty acids have also been developed as PCMs due to their advantageous characteristics such as their availability, low cost, and renewability. Despite the numerous studies available in the literature with organic PCMs, they are not focused on low temperature energy storage applications, and this can be attributed to the lack of information concerning essential characteristics as the fusion temperature range and their thermophysical properties, such as the thermal conductivity. Thus, the search for new suitable organic PCMs for cold TES systems is becoming crucial to fulfil the needs for the desired applications [19, 21]. Regarding this, *n*-alkyl adipates, and other esters, have been recently started to be studied and proved to be viable PCMs for TES applications at low temperatures [21–23]. Additionally, they also present suitable properties for industrial applications such as low cost, low toxicity and chemical stability, and are considered to be environmentally friendly [24, 25].

This work aims to the characterization of a selected system of two di-*n*-alkyl-adipates that can be used for energy storage at low temperatures, starting by the construction of solid–liquid phase diagrams using DSC and Raman spectroscopy studies. In addition, to the best of our knowledge, no research studies exploring binary system of diethyl and dibutyl adipates, for cool thermal storage applications, has been reported in the literature.

2 Experimental

2.1 Materials

Diethyl adipate was supplied by Sigma Aldrich, Lot number STBD3299V, with a purity > 99.9 %, according to the Certificate of Analysis. Dibutyl adipate was supplied by TCI Chemicals, Lot number SG2JN-ML, with a purity of 99.9 %, according to the corresponding Certificate of Analysis.

The water content of the materials used in this work were measured using a Karl-Fisher 831 KF Coulometer from Metrohm. The values of water content were 617.4 ppm for diethyl adipate and 6.8 ppm for dibutyl adipate.

2.2 Experimental Techniques

2.2.1 Differential Scanning Calorimetry (DSC)

The calorimetric measurements were performed with a 2920 MDSC system from TA Instruments Inc. The sample masses of 3.0–10.0 mg were sealed in air inside aluminium pans, weighed with a precision of ± 0.1 μg in a Mettler UMT2 ultra-micro balance and analysed at a scanning rating of $\beta = 5$ K·min^{-1}. Helium (Air Liquide N55), at a flow rate of 30 cm^3 min^{-1} was used as purging gas. The baseline was corrected by scanning the temperature range of the experiments with an empty pan.

The temperature and heat flow scales of the instrument were calibrated at different heating rates, based on the onsets of the fusion peaks of several standards. Details of the calibration are described and presented elsewhere [26]. The software used was TA Universal Analysis 2000 v4.0.

2.2.2 Hot Stage Microscopy (HSM)

Polarized optical microscopy observations were performed on an Olympus BX51 optical microscope. The temperature changes and stabilization were set by a Linkam LTS360 liquid nitrogen cooled cryostage and was measured with a Pt resistance thermometer. The liquid samples were first placed on the glass plate, covered by a second glass and cooled down at 5 K·min^{-1}. After solidification, the microstructure of the sample was monitored with an Olympus C5060 wide zoom camera for picture and/or movie record. Images were recorded with 250× magnification in the temperature range from 183.15 K to 293.15 K at a heating rate of 5 K·min^{-1}.

2.2.3 Raman Spectroscopy

The Raman spectra were obtained using a micro-Raman Horiba LabRam HR Evolution system, with excitation provided by a 532 nm solid-state laser, using an approximate power of 50 mW at the sample. A 50× long working distance objective was used, with a laser spot diameter of around 1 μm in the sample. The equipment was calibrated using a Si crystal (reference band at 520.5 cm^{-1}). The final spectra were the average of 5 spectra accumulations obtained with an acquisition-time of 5 s and resolution of 0.5 cm^{-1}. A hot stage THMS 600 (Linkam Scientific Instruments), controlled by a T95-PE Linkpad controlling unit, was used for the temperature-variation Raman experiments.

3 Results and Discussion

3.1 Differential Scanning Calorimetry (DSC)

DSC heating curves of the pure compounds, diethyl adipate and dibutyl adipate and some of the most significant binary mixtures are presented in Fig. 1. The relevant temperatures and enthalpies of fusion were obtained using the average of two corresponding values for each cycle and are given in Table 1; the supplementary material contains the remaining DSC curves in Fig. S1, and the corresponding temperature and enthalpy of fusion values in Table S1.

The curves shown in Fig. 1 evidence two different types of solid–liquid transition. In the case of pure compounds and the eutectic mixture, only a single peak corresponding to the fusion is detectable while for the mixtures with molar fraction $x_{\text{dibutyl}} = 0.80$ and $x_{\text{dibutyl}} = 0.20$ it is possible to identify two distinct peaks; also, for the mixture with $x_{\text{dibutyl}} = 0.20$ the peak assigned to the polymorphism of dibutyl adipate is detectable. Nonetheless, the temperature of the polymorphic transition is always the same and does not affect the solid–liquid
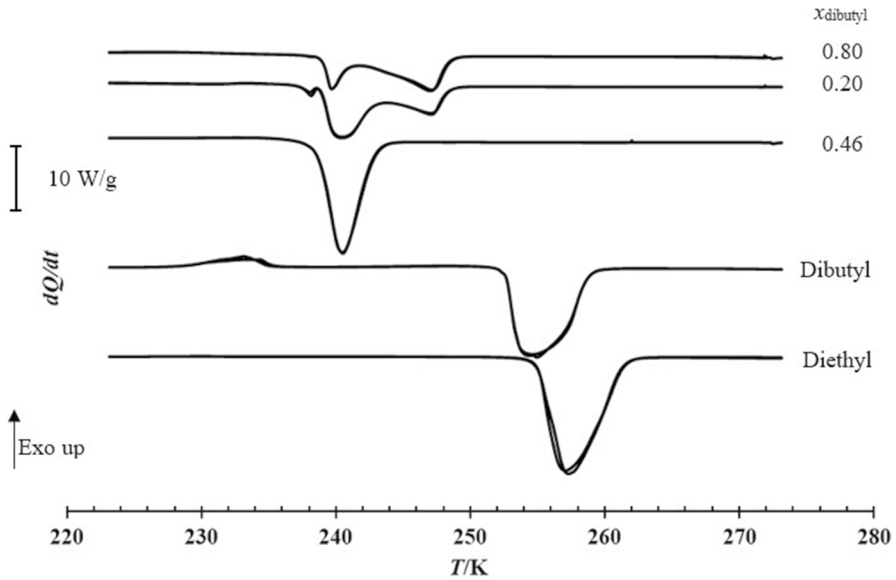
Fig. 1 DSC heating curves of pure diethyl, dibutyl, and of selected binary mixtures, with dibutyl molar fraction $x_{dibutyl}$

Table 1 DSC data of pure diethyl adipate, pure dibutyl adipate and three of their binary mixtures

$x_{dibutyl}$	DSC 1st peak			DSC 2nd peak		
	T_{onset} /K	T_{max} /K	$\Delta_{fus}H$ /J·g^{-1}	T_{onset} /K	T_{max} /K	$\Delta_{fus}H$ /J·g^{-1}
0	–	–	–	251.51	253.55	102.8
0.20	238.95	240.15	46.18	244.64	247.28	17.12
0.46	–	–	–	238.67	240.46	131.7
0.80	239.00	239.63	27.57	243.52	247.17	68.36
1	–	–	–	249.08	251.17	153.1

phase transition for any of the studied mixtures, including the eutectic mixture which is the most interesting one in terms of TES application. These results enable to rationalise the different shape of the curves according to the molar fraction of diethyl adipate.

Concerning the pure components, it was observed that diethyl adipate melts at $T_{max} = 253.55$ K with an enthalpy of fusion, $\Delta_{fus}H = 102.8$ J·g^{-1} and dibutyl adipate melts at 251.17 K with $\Delta_{fus}H = 153.1$ J·g^{-1}. A eutectic mixture is found with molar fraction $x_{dibutyl} = 0.46$ with a eutectic temperature $T_{max} = 240.46$ K with an enthalpy of fusion, $\Delta_{fus}H = 131.7$ J·g^{-1}. Furthermore, it has been observed that dibutyl adipate presents polymorphism, being the polymorph

1 transformed into polymorph 2 at ca. 238.15 K on heating, with an enthalpy around $\Delta_{trans}H = 2.50 \text{ J·g}^{-1}$.

These preliminary findings obtained from isolated DSC experiments, have been complemented by Hot Stage Microscopy and needed confirmation using another sort of instrumentation and studies, like low temperature Raman spectroscopy.

3.2 Hot Stage Microscopy

Hot stage microscopy enabled to verify the results obtained using DSC. By employing light polarization, it was possible to observe not only the solid–liquid phase transition, but also the polymorphic transition. In Fig. 2, it is possible to visualize two different cases: (a) the polymorphism of dibutyl adipate for the eutectic sample and, (b) the phase transition for the $x_{dibutyl} = 0.10$ mixture.

In the first case, Fig. 2a, the mixture $x_{dibutyl} = 0.1$ reveals that a partial phase transition with the appearance of some drops of liquid first occurs, and that this mixture of solid and liquid phases continues to evolve until there is only the liquid phase. In Fig. 2b, the eutectic mixture is shown, where not only it is possible to see the polymorphic transition of dibutyl adipate by the change of form, with concomitant colour modification of the solid, but also the sudden phase transition similar to a pure compound, a typical signature of a eutectic transition.

3.3 Raman Spectroscopy

Raman spectra of pure diethyl adipate and dibutyl adipate for both solid and liquid phases, of the eutectic mixture and of one binary mixture having $x_{dibutyl} = 0.20$ for different temperatures are presented in Figs. 3, 4, 5 and 6, respectively; being the
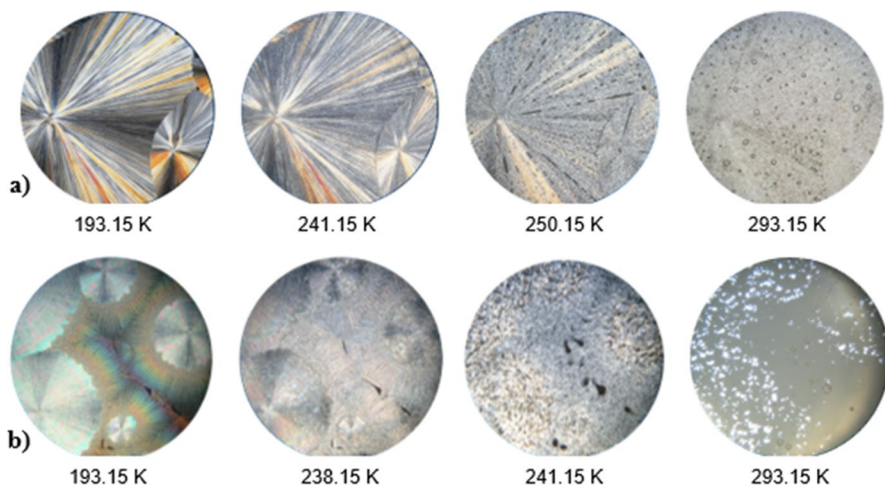

Fig. 2 Hot stage microscopy results for the $x_{dibutyl} = 0.1$ mixture (a) and for the eutectic mixture (b) in temperature region between 193.15 K and 293.15 K, with 250× magnification
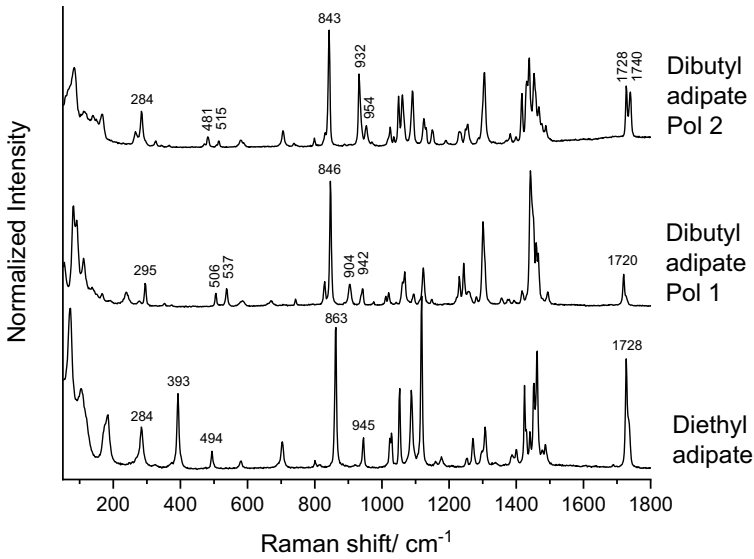
Fig. 3 Raman spectra for the solid-state pure diethyl adipate and dibutyl adipate samples
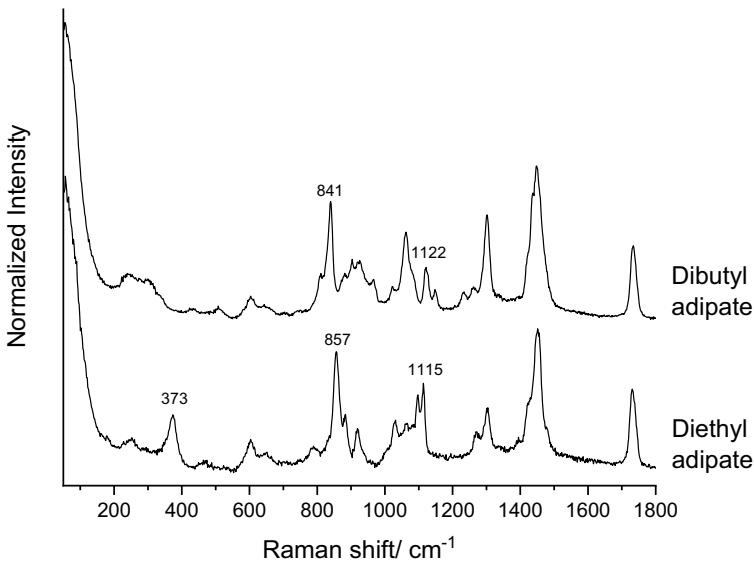

Fig. 4 Raman spectra of room-temperature liquid samples of diethyl adipate and dibutyl adipate

remaining Raman spectra demonstrated in Figs. S2, S3 and S4 in the supplementary information. Additionally, the Raman equipment enabled to obtain images of the system during the experiments, which is particularly significant to monitor the system in real time and corroborate visually the results obtained using DSC. These
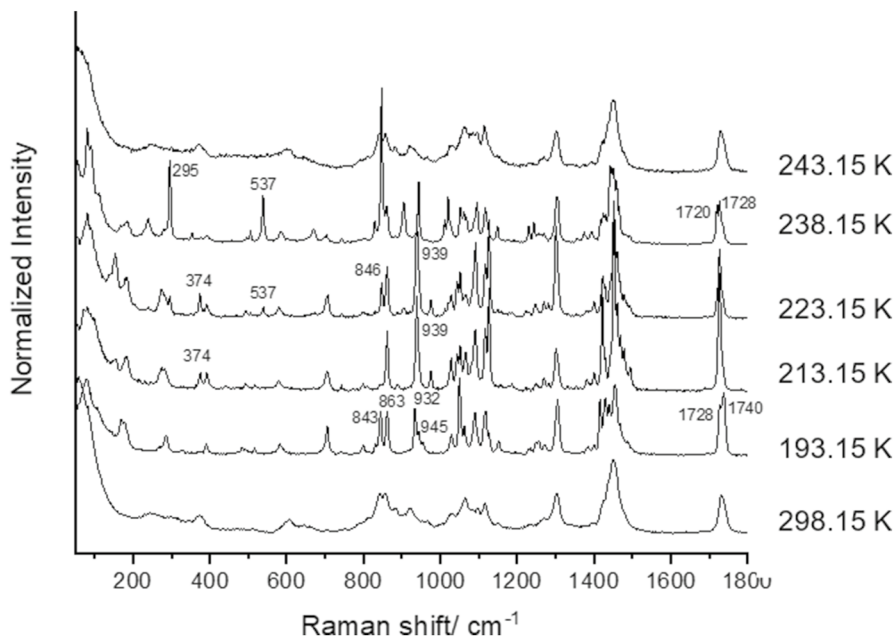
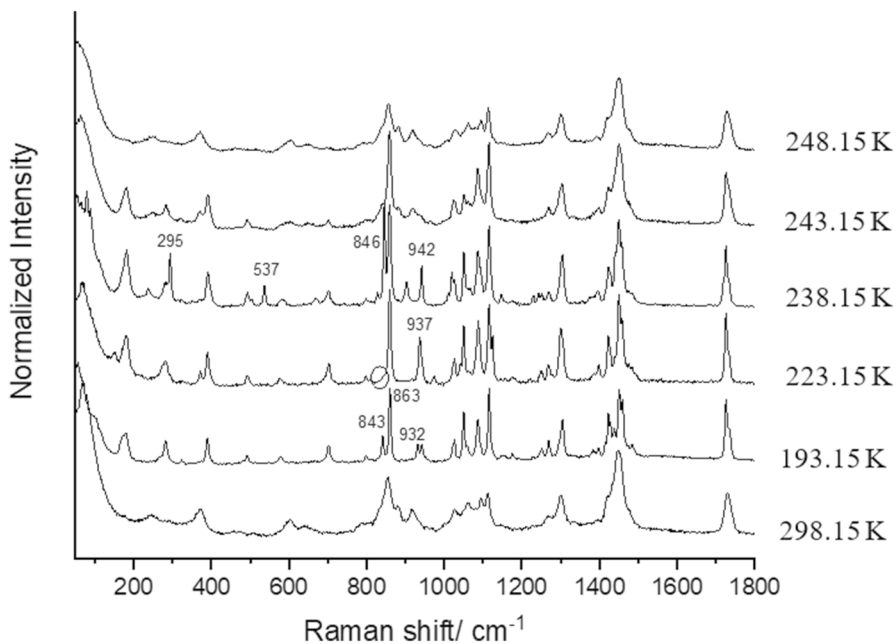**Fig. 5** Temperature-variation Raman spectra for the eutectic binary mixture sample

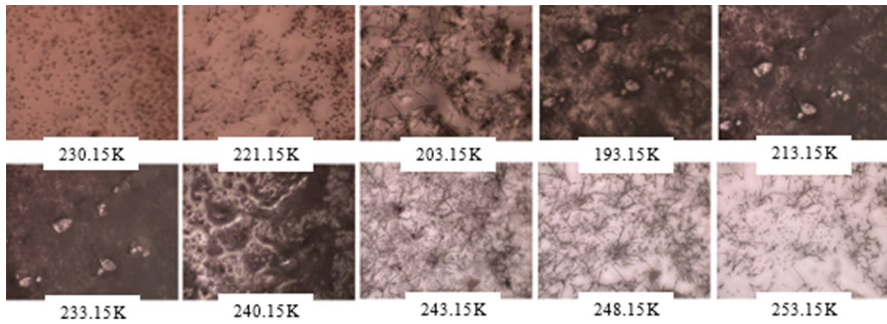**Fig. 6** Temperature-variation Raman spectra for the $x_{\text{dibutyl}} = 0.20$ sample

Fig. 7 Eutectic mixture photographs collected during the temperature-variation Raman spectroscopy experiment, with 10× magnification

images are presented in Figs. 7 and 8 for the eutectic mixture and the binary mixture with $x_{dibutyl} = 0.20$, respectively; additionally, the surplus images for other mixtures are in the supplementary information in Figs. S5, S6, S7 and S8. The results for pure diethyl and dibutyl adipates in solid and liquid-state enable to identify the marker bands for each compound. The polymorphism of dibutyl adipate was confirmed at 238 K. The eutectic mixture has a sharp melting point, contrary to what is observed for the system with overall composition $x_{dibutyl} = 0.20$.

The temperature-variation Raman experiment on the eutectic mixture shows that both the diethyl adipate (e.g., 863 cm^{-1}, 945 cm^{-1} and 1728 cm^{-1}) and the dibutyl adipate polymorph 2 (843 cm^{-1}, 932 cm^{-1} and 1740 cm^{-1}) marker bands are identified at 193.15 K. At 213.15 K the marker bands of dibutyl adipate polymorph 2 are no longer present (843 cm^{-1}, 932 cm^{-1} and 1740 cm^{-1}). At 223.15 K the 537 cm^{-1} and 846 cm^{-1} marker bands of dibutyl adipate polymorph 1 are already observed. At 238.15 K, the marker bands of dibutyl adipate polymorph 1 reach their highest intensity values, and at 243.15 K the collected spectrum resembles the one of the liquid-state sample.

For the $x_{dibutyl} = 0.20$ mixture at 193.15 K, the marker bands of diethyl adipate (e.g., 863 cm^{-1}) and dibutyl adipate polymorph 2 (e.g., 843 cm^{-1} and 932 cm^{-1}) are clearly identifiable. At 223.15 K, the dibutyl adipate polymorph 2 disappears (as
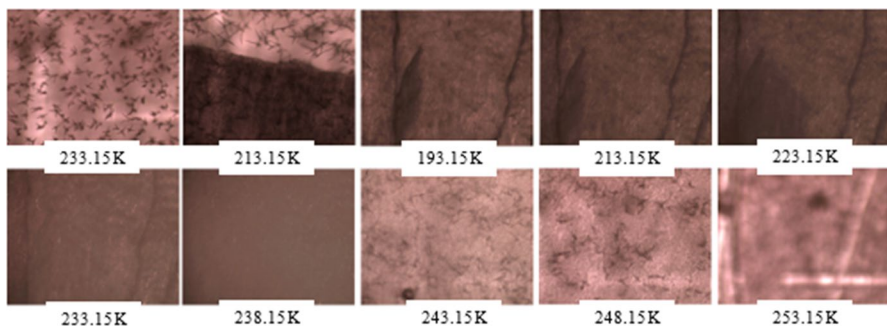

Fig. 8 80:20 diethyl adipate:dibutyl adipate mixture photographs collected during the temperature-variation Raman spectroscopy experiment, with 10× magnification

identified by the circle in Fig. 6) and a new band at 937 cm^{-1} appears, which might indicate the evolution of dibutyl adipate polymorph 2 into polymorph 1. At 238.15 K, the marker bands of dibutyl adipate polymorph 1 (e.g., 295 cm^{-1}, 537 cm^{-1}, 846 cm^{-1} and 942 cm^{-1}) are identified, meaning that the polymorph ($2\rightarrow1$) transition is fully completed at this temperature. At 243.15 K, the dibutyl adipate polymorph 1 marker bands are no longer present, corresponding to the complete melting of this compound, and the marker bands of diethyl adipate start to broaden, corresponding to the beginning of the melting process of this solid, which is completed at 248.15 K.

3.4 Solid–Liquid Binary Phase Diagram

The DSC thermograms and the complementary studies carried out using Hot Stage Microscopy and, especially, Low Temperature Raman Spectroscopy results have led to the construction of a solid–liquid phase diagram for the system (dibutyl adipate + diethyl adipate) as shown in Fig. 9. This phase diagram was obtained using the experimental results for 30 different molar fractions of the binary mixture and for the two pure components. It is possible to identify two
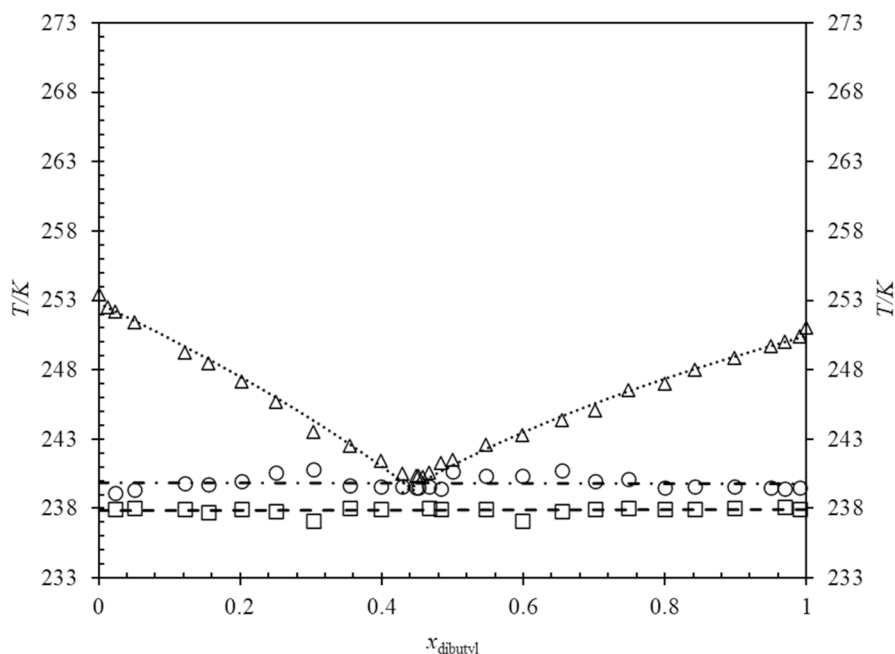

Fig. 9 Binary solid–liquid phase diagram of the system of diethyl and dibutyl adipates; •• *liquidus* fitting curve according to the Eq. 2, Δ experimental *liquidus* line data points, –·– *solidus* line, ○ experimental *solidus* line data points, ▪▪ ▪ polymorphic line, □ experimental polymorphic transition temperature data points

biphasic zones where solid and liquid coexist: one liquid solution in equilibrium with different solid phases, determined by the overall composition of the system.

The freezing-point depression curve can, in principle, be used to characterise the *liquidus* line of a solid–liquid binary phase diagram of a non-isomorphous eutectic system [19]. It can be described by Eq. 1, where x is the molar fraction, T is the *liquidus* temperature for molar fraction x, T_{Mi} and L_{Mi} are the temperature and enthalpy of melting of the pure compound i, respectively, and R is the gas constant. This equation results from assuming that: the two components of an ideal liquid solution do not form solid solutions with each other; the ideal solution is in equilibrium with one or the other of the pure solid phases and that L is independent of the temperature [27]. This same equation has been previously used by other authors, e.g., Campanella et al. [20], Cortesão et al. [28], and Han et al. [29], for that purpose.

$$\ln\left(\frac{1}{x}\right) = \frac{L_{Mi}}{R}\left(\frac{1}{T} - \frac{1}{T_{Mi}}\right) \tag{1}$$

In the present work, the liquidus line was obtained by a fitting procedure, making use of all the experimental points obtained in the DSC studies. These 32 experimental points cover the whole range of compositions, including the fusion points for the pure components, and 30 binary mixtures. For that purpose, it was decided that an equal statistical weight should be attributed to all the data, including the fusion temperatures of the pure components. Therefore, Eq. 2 has been applied to define the *liquidus* line of the present system, as shown in Fig. 9.

$$\ln\left(\frac{1}{x}\right) = a + b \cdot \frac{1}{T} \tag{2}$$

Equation 2 is derived from Eq. 1, letting both L_{Mi} and T_{Mi} lose their precise original physical significance and be included in the fitting parameters, a and b, and can be estimated by Eqs. 3 and 4, for comparison.

$$a = -\frac{L_{Mi}}{R} \cdot \frac{1}{T_{Mi}} \tag{3}$$

$$b = \frac{L_{Mi}}{R} \tag{4}$$

The *liquidus* line obtained using the fitting Eq. 2 shows an excellent agreement with the 32 experimental data points obtained by differential scanning calorimetry; the coordinates of the eutectic point being well predicted by the intersection of Eq. 2, when applied to each side of the diagram, as depicted in Fig. 9.

The experimental *solidus* and *liquidus* temperature points were obtained from the maximum of the first and second endothermic peaks in the DSC curves, respectively. Figure 10 shows the deviations of the thermal analysis experimental data from the correlation Eq. 2, using the parameters in Table 2. The maximum absolute deviation of all data are smaller than ± 1.5 K.
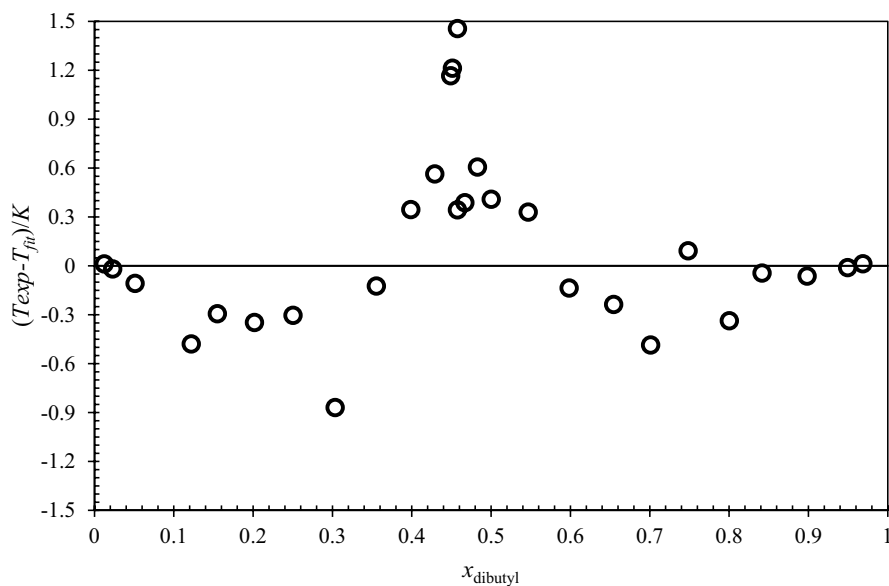
Fig. 10 Absolute deviations of the experimental data obtained with thermal analysis, from the fitting Eq. 2, as a function of dibutyl adipate molar fraction

Table 2 Fitting parameters a and b of Eq. 2 and the correspondent relative root mean square deviation σ_R for the experimental *liquidus* data points using DSC

Left side of the diagram			Right side of the diagram		
a	b/K	σ_R/%*	a	b/K	σ_R/%*
− 10.5	2.65×10^3	0.25	− 17.9	4.49×10^3	0.13

*Defined in the Supplementary information

Table 3 Comparison of the results obtained by fitting for L_{Mi} and T_{Mi} and the experimental results of $\Delta_{fus}H$ and T_{fus} for pure diethyl and dibutyl adipates

Diethyl adipate			Dibutyl adipate		
L_{Mi}/J·g^{-1}	$\Delta_{fus}H$/J·g^{-1}	Dev./J·g^{-1}	L_{Mi}/J·g^{-1}	$\Delta_{fus}H$/J·g^{-1}	Dev./J·g^{-1}
109.1	102.8	6.3	144.6	153.1	− 8.5
T_{Mi}/K	T_{fus}/K	Dev./K	T_{Mi}/K	T_{fus}/K	Dev./K
252.95	253.55	− 0.60	250.58	251.17	− 0.59

According to Eqs. 3 and 4, it is possible to estimate the values for L_{Mi} and T_{Mi} from the fitting parameters *a* and *b*. In Table 3 the values of L_{Mi} and T_{Mi} obtained by the fitting of Eq. 2 are compared to the experimental values of $\Delta_{fus}H$ and T_{fus} for pure diethyl and dibutyl adipates.

Additionally, the eutectic composition and temperature were calculated by the intersection of the two fitted *liquidus* lines for each side of the binary phase diagram. According to the fitting Eq. 2, the eutectic composition, $x_{dibutyl}$, is 0.44 and the eutectic temperature is $T_{fus} = 239.78$ K, which corresponds to an absolute deviation of 0.68 K compared to the experimental result. The root mean square deviation of the experimental data points to the fitting equation for the *liquidus* line, hereby designated as σ, was determined as 0.54 K. Therefore, the uncertainty is well within a 0.95 confidence level.

4 Conclusions

Organic PCMs have been under massive research due to their high latent heat enthalpy and chemical stability. In particular non-paraffin-based compounds have, recently, shown good potential as PCMs for TES applications supported by the availability, low cost and renewability. Although, these studies are not focused on low temperature energy storage applications and, thus, the search for new suitable organic PCMs for cold TES systems is becoming crucial to fulfil the needs for the desired applications.

In the present article, a binary system of two di-*n*-alkyl adipates, in particular, diethyl and dibutyl adipates, is characterized in order to be used for low temperature energy storage applications. DSC tests performed with 30 different mole fractions of the binary mixture, complemented with studies achieved by Raman spectroscopy with temperature-variation allowed the detailed construction of the solid–liquid phase diagram for this system. Additionally, the *liquidus* curve of the phase diagram was also successfully described using a suitable fitting equation. The studied binary system reveals eutectic behaviour at low temperatures, being the eutectic temperature found at 240.46 K with a molar fraction $x_{dibutyl} = 0.46$ and an enthalpy of fusion $\Delta_{fus}H = 131.7$ J·g^{-1}. The characteristic polymorphic transition of dibutyl adipate is also observed in the binary mixtures at around 238 K with an enthalpy value of $\Delta_{trans}H = 2.50$ J·g^{-1}. The optical image of the polymorphic transition, under polarized light, was also identified by HSM.

In summary, the present studied binary system of di-*n*-alkyl adipates proved to be a good candidate as PCM for TES applications at low temperatures. As far as the authors are aware, no low temperature TES research studies for the present binary system, has been reported in the literature.

Future work will be focused on the study of the thermophysical properties of this binary system, e.g., the thermal conductivity, which is imperative for the practical application as PCM.

Declarations

Competing interests The authors declare that they have no competing financial interest or personal relationships that could have appeared to influence the work reported in this paper.

References

1. C. Liu, F. Li, M. Lai-Peng, H.M. Cheng, Advanced materials for energy storage. Adv. Mater. **22**, 28–62 (2010). https://doi.org/10.1002/adma.200903328
2. O.E. Ataer, Storage of thermal energy, in *Encyclopedia of Life Support Systems* (Eolss Publishers, Oxford, 2006), pp. 25–32.
3. S. Koohi-Fayegh, M.A. Rosen, A review of energy storage types, applications and recent developments. J. Energy Storage. **27**, 101047 (2019). https://doi.org/10.1016/j.est.2019.101047
4. E. Oró, A. de Gracia, A. Castell, M.M. Farid, L.F. Cabeza, Review on phase change materials (PCMs) for cold thermal energy storage applications. Appl. Energy **99**, 513–533 (2012). https://doi.org/10.1016/j.apenergy.2012.03.058
5. A. Sharma, V.V. Tyagi, C.R. Chen, D. Buddhi, Review on thermal energy storage with phase change materials and applications. Renew. Sustain. Energy Rev. **13**, 318–345 (2019). https://doi.org/10.1016/j.rser.2007.10.005
6. E.B.S. Mettawee, G.M.R. Assassa, Thermal conductivity enhancement in a latent heat storage system. Sol. Energy **81**, 839–845 (2007). https://doi.org/10.1016/j.solener.2006.11.009
7. E. Günther, S. Hiebler, H. Mehling, R. Redlich, Enthalpy of phase change materials as a function of temperature: Required accuracy and suitable measurement methods. Int. J. Thermophys. **30**, 1257–1269 (2009). https://doi.org/10.1007/s10765-009-0641-z
8. D.G. Atinafu, S. Jin Chang, K.H. Kim, S. Kim, Tuning surface functionality of standard biochars and the resulting uplift capacity of loading/energy storage for organic phase change materials. Chem. Eng. J. **394**, 125049 (2020). https://doi.org/10.1016/j.cej.2020.125049
9. L.F. Cabeza, E. Oró, Thermal energy storage for renewable heating and cooling systems, in *Renewable Heating and Cooling* (Elsevier, Amsterdam, 2016), pp. 139–179. https://doi.org/10.1016/B978-1-78242-213-6.00007-2
10. C. Veerakumar, A. Sreekumar, Phase change material based cold thermal energy storage: materials, techniques and applications—a review. Int. J. Refrig. **67**, 271–289 (2016). https://doi.org/10.1016/j.ijrefrig.2015.12.005

11. Y. Lin, Y. Jia, G. Alva, G. Fang, Review on thermal conductivity enhancement, thermal properties and applications of phase change materials in thermal energy storage. Renew. Sustain. Energy Rev. **82**, 2730–2742 (2018). https://doi.org/10.1016/j.rser.2017.10.002

12. D. Zhou, C.Y. Zhao, Y. Tian, Review on thermal energy storage with phase change materials (PCMs) in building applications. Appl. Energy **92**, 593–605 (2012). https://doi.org/10.1016/j.apenergy.2011.08.025

13. T. Shen, S. Li, H. Peng, X. Ling, Experimental study and thermodynamic modeling of solid-liquid equilibrium of binary systems: dodecane-tetradedcane and tridecane-pentadecane for cryogenic thermal energy storage. Fluid Phase Equilib. **493**, 109–119 (2019). https://doi.org/10.1016/j.fluid.2019.04.023

14. I. Sarbu, C. Sebarchievici, *Solar Heating and Colling Systems*, 1st edn. (Academic Press, New York, 2017)

15. B.E. Jebasingh, A.V. Arasu, Characterisation and stability analysis of eutectic fatty acid as a low cost cold energy storage phase change material. J. Energy Storage **31**, 101708 (2020). https://doi.org/10.1016/j.est.2020.101708

16. B. Nie, A. Palacios, B. Zou, J. Liu, T. Zhang, Y. Li, Review on phase change materials for cold thermal energy storage applications. Renew. Sustain. Energy Rev. **134**, 110340 (2020). https://doi.org/10.1016/j.rser.2020.110340

17. A. Sari, C. Alkan, D. Kahraman Döğüşcü, A. Biçer, Micro/nano-encapsulated n-heptadecane with polystyrene shell for latent heat thermal energy storage. Sol. Energy Mater. Sol. Cells **126**, 42–50 (2014). https://doi.org/10.1016/j.solmat.2014.03.023

18. Y. Li, D. Yang, J. Xie, J. Wang, Review on research and application of phase change materials in cold storage refrigerator. IOP Conf. Ser. Earth Environ. Sci. (2021). https://doi.org/10.1088/1755-1315/766/1/012094

19. S.N. Gunasekara, V. Martin, J.N. Chiu, Phase equilibrium in the design of phase change materials for thermal energy storage: state-of-the-art. Renew. Sustain. Energy Rev. **73**, 558–581 (2017). https://doi.org/10.1016/j.rser.2017.01.108

20. L. Campanella, V. Micieli, M. Tomassetti, S. Vecchio, Solid-liquid phase diagrams of binary mixtures: acetylsalicylic acid(1) + E(2) (E = salicylic acid, polyethylene glycol 4000, d-mannitol). J. Therm. Anal. Calorim. **99**, 887–892 (2010). https://doi.org/10.1007/s10973-010-0680-5

21. G.V.N. Trivedi, R. Parameshwaran, Micro/nanoencapsulation of dimethyl adipate with melamine formaldehyde shell as phase change material slurries for cool thermal energy storage. Chem. Thermodyn. Therm. Anal. (2022). https://doi.org/10.1016/j.ctta.2022.100037

22. B. Al-Aifan, R. Parameshwaran, K. Mehta, R. Karunakaran, Évaluation de la Performance d'un olume De Frigorigène Variable Combiné À un Système de Stockage d'Énergie Thermique Froide Pour des Applications de Conditionnement D'Air. Int. J. Refrig. **76**, 271–295 (2017). https://doi.org/10.1016/j.ijrefrig.2017.02.008

23. K. Pielichowska, K. Pielichowski, Phase change materials for thermal energy storage. Prog. Mater. Sci. **65**, 67–123 (2014). https://doi.org/10.1016/j.pmatsci.2014.03.005

24. M.J.P. Comuñas, J.P. Bazile, L. Lugo, A. Baylaucq, J. Fernández, C. Boned, Influence of the molecular structure on the volumetric properties and viscosities of dialkyl adipates (dimethyl, diethyl, and diisobutyl adipates). J. Chem. Eng. Data **55**, 3697–3703 (2010). https://doi.org/10.1021/je100237h

25. ŞI. Kirbaşlar, E. Ince, S. Şahin, U. Dramur, (Liquid + liquid) equilibria of (water + propionic acid + dibasic esters) ternary systems. J. Chem. Thermodyn. **39**, 1493–1499 (2007). https://doi.org/10.1016/j.jct.2007.02.012

26. J.J. Moura Ramos, R. Taveira-Marques, H.P. Diogo, Estimation of the fragility index of indomethacin by DSC using the heating and cooling rate dependency of the glass transition. J. Pharm. Sci. **93**, 1503–1507 (2004). https://doi.org/10.1002/jps.20061

27. K. Denbigh, *Principles of Chemical Equilibrium*, 2nd edn. (Cambridge University Press, London, 1966)

28. A.M. Cortesão, J.G. Henriques, R.A.E. Castro, T.M.R. Maria, J. Canotilho, M.E.S. Eusébio, Binary phase diagrams of pyridinecarboxamide isomers. J. Therm. Anal. Calorim. **130**, 1727–1733 (2017). https://doi.org/10.1007/s10973-017-6474-2

29. L. Han, G. Ma, S. Xie, J. Sun, Y. Jia, Y. Jing, Thermal properties and stabilities of the eutectic mixture: 1,6-hexanediol/lauric acid as a phase change material for thermal energy storage. Appl. Therm. Eng. **116**, 153–159 (2017). https://doi.org/10.1016/j.applthermaleng.2017.01.082

Authors and Affiliations

Maria C. M. Sequeira[1] · **Bernardo A. Nogueira[2]** · **Fernando J. P. Caetano[1,3]** · **Hermínio P. Diogo[1]** · **João M. N. A. Fareleira[1]** · **Rui Fausto[2,4]**

✉   Fernando J. P. Caetano
     fernando.caetano@uab.pt

✉   Hermínio P. Diogo
     hdiogo@tecnico.ulisboa.pt

[1]   Centro de Química Estrutural, Institute of Molecular Sciences, Departamento de Engenharia Química, Instituto Superior Técnico, Universidade de Lisboa, Av. Rovisco Pais, 1049 001 Lisbon, Portugal

[2]   CQC-IMS, Departamento de Química, Universidade de Coimbra, 3004-535 Coimbra, Portugal

[3]   Departamento de Ciências e Tecnologia, Universidade Aberta, Lisbon, Portugal

[4]   Department of Physics, Faculty of Sciences and Letters, Istanbul Kultur University, Ataköy Campus, 34156 Bakirköy, Istanbul, Turkey